

Galactic Cosmic-Ray Composition and Spectra for Ne through Cu from 0.8 to 10 GeV/nuc with the SuperTIGER Instrument

A. W. Labrador^{1,*}, W. R. Binns², T. J. Brandt³, T. Hams^{3,6}, M. H. Israel², J. T. Link^{3,6}, R. A. Mewaldt¹, J. W. Mitchell³, R. P. Murphy², B. F. Rauch², K. Sakai^{3,6}, M. Sasaki^{3,6}, E. C. Stone¹, C. J. Waddington⁴, J. E. Ward^{2,7}, M. E. Wiedenbeck⁴

¹ California Institute of Technology, Pasadena, CA 91125 USA

² Washington University, St. Louis, MO 63130 USA

³ NASA/Goddard Space Flight Center, Greenbelt, MD 20771 USA

⁴ The University of Minnesota, Minneapolis, MN 55455, USA

⁵ Jet Propulsion Laboratory, California Institute of Technology, Pasadena, CA 91109 USA

⁶ Center for Research and Exploration in Space Science and Technology (CRESTT), Greenbelt, MD 20771, USA

⁷ Institut de Fisica d'Altes Energies (IFAE), Bellaterra, Spain

E-mail: labrador@srl.caltech.edu

SuperTIGER (Trans-Iron Galactic Element Recorder) is a large-area balloon-borne instrument built to measure the galactic cosmic-ray abundances of elements from $Z=10$ (Ne) through $Z=56$ (Ba) at energies from 0.8 to ~ 10 GeV/nuc. SuperTIGER successfully flew around Antarctica for a record-breaking 55 days, from December 8, 2012 to February 1, 2013. In this paper, we present results of an analysis of the data taken during the flight for elements from $Z=10$ (Ne) to $Z=28$ (Ni). We report excellent charge separation throughout this range, with an Fe charge resolution of 0.16 charge units. Using a small sample of our data ($\sim 1/40$ th of our total), we will compare our galactic element secondary to primary ratios (e.g. (Sc+Ti+V)/Fe) with those from other instruments operating at different energy ranges.

* Speaker

The 34th International Cosmic Ray Conference

30 July- 6 August, 2015

The Hague, The Netherlands

1. Introduction

SuperTIGER (Trans-Iron Galactic Element Recorder) is a large-area balloon-borne instrument built to measure the galactic cosmic-ray abundances of elements from $Z=10$ (Ne) through $Z=56$ (Ba) for energies >0.8 GeV/nuc and energy spectra over the range 0.8 to 10 GeV/nuc. SuperTIGER successfully flew around Antarctica for a record-breaking 55 days, from December 8, 2012 to February 1, 2013.

A primary goal of SuperTIGER is the measurement of ultra-heavy ($Z \geq 30$) cosmic ray abundances in order to compare with models of galactic cosmic ray (GCR) transport and origin, particularly in OB associations [1-5]. However, SuperTIGER also measured element data from $Z=10$ (Ne) to $Z=29$ (Cu) with excellent charge resolution allowing multiple additional areas for investigation. Secondary-to-primary ratios in GCRs have long been used to measure the pathlength of matter traversed by those cosmic rays during propagation in the galaxy, and SuperTIGER's measurements of secondary-to-primary ratios may be used to distinguish between different cosmic ray propagation models. Additionally, the energy resolution in SuperTIGER should be sufficient to detect possible signatures of microquasars in Fe energy spectra [6].

In this paper, we discuss the particle identification and energy measurements for elements with $Z=10-29$, report preliminary secondary/primary ratios, and compare the ratios to those measured by other instruments and to predictions of a GCR transport model. For reasons relating to a priority system described below, we limit the data analyzed for this paper to a subset representing 1/40th of our total data set.

2. The SuperTIGER Instrument

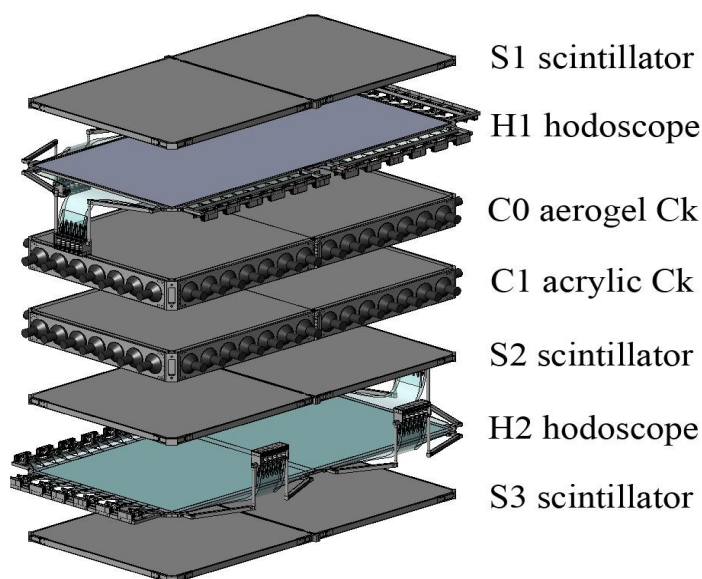


Figure 1: An expanded view of one module of SuperTIGER. Figure taken from Binns et al. [1].

The SuperTIGER instrument is divided into two nearly identical modules, each of which is a stack of several detectors. From top to bottom, the detectors in each module are a plastic scintillator (S1), a top scintillating optical fiber hodoscope (H1), an aerogel Cherenkov (refractive index $n=1.025$ or $n=1.043$) detector (C0), an acrylic Cherenkov ($n=1.49$) detector (C1), another plastic scintillator (S2), a bottom hodoscope (H2), and a third plastic scintillator (S3). In one module, the aerogel blocks in the C0 detector are entirely $n=1.043$ refractive index aerogels (or a threshold energy of ~ 2.5 GeV/nuc), while in the other module, half of the C0 aerogels have a refractive index $n=1.043$ while the other half have $n=1.025$ (threshold ~ 3.3 GeV/nuc). Otherwise, the modules are functionally identical. See Figure 1.

The SuperTIGER instrument is described in greater detail by Binns et al. [2].

3. Data Analysis

Particle identification by charge and velocity is achieved by combinations of measurements from the scintillation and Cherenkov detectors. See Figures 2 and 3. The hodoscopes provide particle trajectories, allowing angle- and position-dependent detector responses to be mapped and corrected for in the data analysis. The S3 scintillator flags particle events that interact in the instrument.

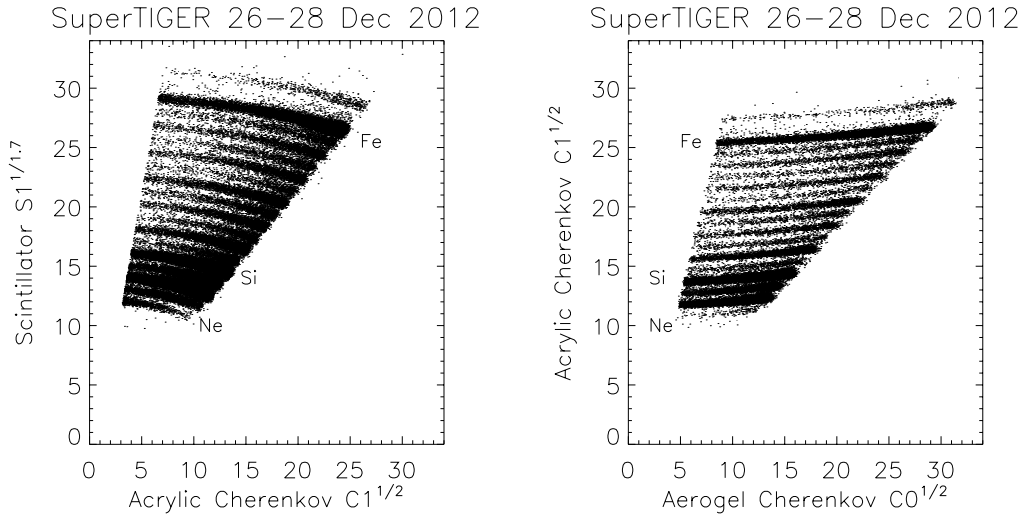


Figure 2: S1 vs. C1 signal (left) and C1 vs. C0 signal (right) showing a sample of SuperTIGER line-of-sight (LOS) flight data below and above C0 threshold energy (~ 2.5 GeV/nuc), respectively

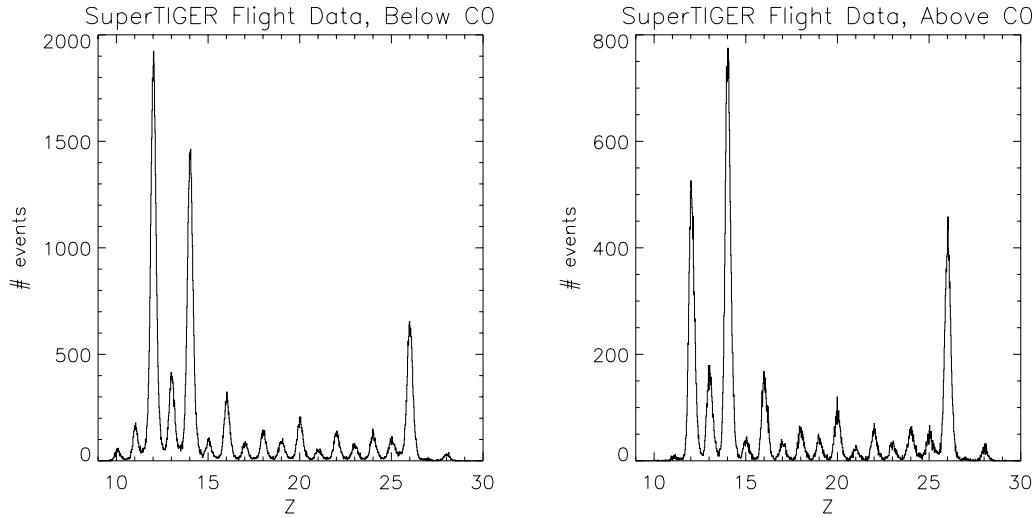


Figure 3: Charge histograms from SuperTIGER flight data for below C0 threshold (left) and above (right). The histograms are plotted with a bin size of 0.02 charge units. The relative difference in charge composition near $Z=10$ can be attributed to higher scintillator signals in the particle trigger at lower energies.

A feature of note in Figure 3 is a much greater relative abundance of low charge (e.g. Ne) events at low energies (below C0 threshold). At our lowest energies, we expect higher scintillator signals for a given charge than at higher energies, so the scintillator trigger thresholds would bias in favor of low charges at low energies. On the other hand, several days after the start of flight, SuperTIGER telemetry incorporated a high/low priority scheme biased in favor of high charges, in particular to ensure transmission of ultra-heavy element data. However, the priority scheme was incorporated only for data transmitted from the payload via satellite (TDRSS), and it was not used for line-of-sight (LOS) data transmission or for onboard storage in solid state drives (SSDs). Additionally, data saved to the SSDs represent a limited fraction of flight data, due to failure of the SSDs during flight. For this paper, we have selected events from LOS data that avoid these biases.

Event selection criteria include fitted trajectories, charge consistency cuts between scintillator detectors, elimination of unphysical events (e.g. Cherenkov signals well above expected maxima for given elements), inconsistent detector responses within individual detectors, and interaction events.

Identification of particles by charge can be achieved easily and directly from the S1 vs. C1 and C1 vs. C0 plots shown in Figure 2, simply by drawing boxes around element tracks in each plot. However, charge identification in this range ($Z=10-29$) is precisely calibrated in order to extend charge identification to ultra-heavy, less-abundant elements ($Z>29$). Charge determination is described in detail by Murphy et al. [4] in these proceedings for the ultra-heavy element analysis, using a model by Voltz et al. [7], with small corrections added to improve fits to SuperTIGER data. The resulting fits

demonstrate SuperTIGER's excellent charge resolution with, for example, the Fe peak showing a charge resolution of 0.16 charge units [3].

The charge identification calculations also allow the fitting of Cherenkov light yield curves to both the scintillator vs. Cherenkov data as well as to the C0 vs. C1 data. Such calibration of the Cherenkov light yields will allow the measurement of above-threshold particle velocities, energies, and eventually energy spectra. That analysis is still ongoing.

4. Results

In order to obtain preliminary (Sc+Ti+V)/Fe ratios for this analysis, we apply additional selection criteria to the flight data. Data were restricted to Module 1, to simplify the C0 Cherenkov cut, simplifying the C0 threshold selection to ~ 2.5 GeV/nuc (for the $n=1.043$ aerogels alone). In order to reduce the degree of instrument and atmospheric corrections, particle data were also restricted to those detected at residual atmospheric overburden ≤ 4.25 g/cm² (average vertical overburden of 3.95 g/cm²) and an incidence angle of less than 30° from vertical. Data were retrieved during and after flight from TDRSS, line-of-sight (LOS) telemetry, and onboard SSD storage. For this analysis, we restricted data to a sample of three days (December 26-28, 2012) of LOS data. These high rate data were not subject to the telemetry priority scheme that biased recorded data in favor of higher charges. This data set represents 1/40th of our total data set: 1/20th of the flight duration, and one module out of two.

For corrections to the top of the instrument (TOI), we employ cross sections and interaction lengths from Nilsen et al. [8] and Westfall et al. [9]. For corrections to the top of the atmosphere (TOA), we employ the same atmospheric correction code that was used for TIGER [10].

Figure 4 shows preliminary (Sc+Ti+V)/Fe ratios from SuperTIGER data for below and above C0 threshold (large closed squares). The energy boundary between the two SuperTIGER points corresponds to the aerogel Cherenkov threshold for $n=1.043$, the lower bound (~ 800 MeV/nuc at the top of the atmosphere) is roughly the acrylic Cherenkov threshold combined with the effect of energy loss to the atmospheric depth of the instrument, and the upper bound (~ 10 GeV/nuc) is an approximate limit imposed by the expected loss of energy resolution in the aerogel Cherenkov detector (C0). The plot points in the figure are at the midpoints of the energy ranges (~ 1.4 and ~ 6 GeV/nuc). The uncertainties for SuperTIGER data shown in the figure are statistical. Systematic uncertainties, including uncertainties from the TOI and TOA calculations are yet to be determined, and energy corrections to TOA are also yet to be completed. Our calculations show that the 21264 Fe counted in this analysis alone, not from the entire flight, represent approximately 58% of the Fe at TOI, and TOI Fe represent approximately 74% of the Fe that propagates from TOA.

Additionally, the (Sc+Ti+V)/Fe ratios for ACE/CRIS data for 129-412 MeV/nuc are shown (open squares), from publicly available level 2 data [11]. The time periods averaged for the ACE/CRIS data were the three Bartels rotation covering Dec 2, 2012 through Feb 20, 2013, overlapping the SuperTIGER flight, as well as averages from Aug 22, 2004 through Sep 3, 2005. The 2004-2005 dates are time periods for which the solar modulation parameters were in the range 600-650 MV, approximately the modulation parameter during the SuperTIGER flight.

The SuperTIGER (Sc+Ti+V)/Fe ratio is consistent with the HEAO measurements in the same energy range [12], as well as with a Standard Leaky Box model calculation, with a modulation parameter of 625 MV [13]. The 0.8-35 GeV/nuc HEAO measurements are at energies that are presumably less sensitive to solar modulation than the ACE/CRIS measurements.

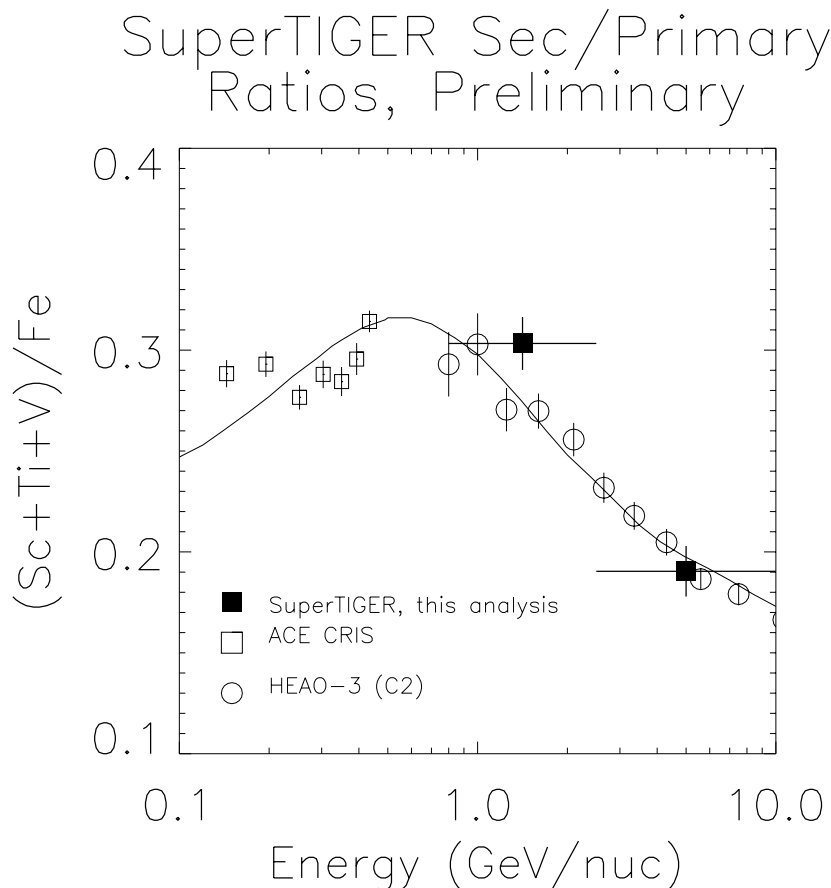


Figure 4: Preliminary sub-iron to iron ratios from SuperTIGER (filled squares). ACE/CRIS data [11] are averaged from the time of the SuperTIGER flight and from time periods in 2004-2005 that had 600-650 MV modulation parameter, similar to the parameter at the time of the SuperTIGER flight. HEAO data are from Engelmann et al. [12]. The curve is a Standard Leaky Box Model curve [13]

5. Conclusion

The SuperTIGER instrument has returned abundant measurements of elements from Ne ($Z=10$) to Cu ($Z=29$) with very good charge resolution. Preliminary analysis of the data yield (Sc+Ti+V)/Fe ratios consistent with measurements from HEAO data and with Standard Leaky Box model calculations. Analysis for the immediate future will focus on expanding the composition analysis to lower charges and on establishing velocity (energy) scales for the Cherenkov data to establish finer energy bins and calculate energy spectra. With energy scales established, we will also be able to trace the energy dependence of the (Sc+Ti+V)/Fe ratios at finer resolution.

Acknowledgements

This work was supported by NASA under grants NNX09AC17G NNX09AC18G, NNX14AB24G, NNX14AB25G, and NNX15AC15G, by the Peggy and Steve Fossett Foundation, and by the McDonnell Center for the Space Sciences at Washington University in St. Louis. We thank the ACE/CRIS instrument team and the ACE Science Center for providing ACE data.

References

- [1] W.R. Binns et al., *Cosmic-Ray Neon, Wolf-Rayet Stars, and the Superbubble Origin of Galactic Cosmic Rays*, The Astrophysical Journal **364** 351 (Nov 2014).
- [2] W.R. Binns et al, *The SuperTIGER Instrument: Measurements of Elemental Abundances of Ultra-Heavy Galactic Cosmic Rays*, The Astrophysical Journal **788** 18 (June 2014).
- [3] M. Hams et al., *SuperTIGER and the Origin of Galactic Cosmic-Rays*, Proc. 34th International Cosmic Ray Conference, The Hague (these proceedings) (2015).
- [4] R. Murphy et al., *Abundances of Ultra-Heavy Galactic Cosmic Rays from the SuperTIGER Instrument*, Proc. 34th International Cosmic Ray Conference, The Hague (these proceedings) (2015).
- [5] B.F. Rauch et al., *Cosmic Ray origin in OB Associations and PReferential Acceleraiton of Refractory Elements: Evidence from Abundances of Elements ^{26}Fe through ^{34}Se* , The Astrophysical Journal **697** 2083 (2009).
- [6] S. Heinz & R. Sunyaev, *Cosmic rays from microquasars: A narrow component to the CR spectrum?*, Astronomy and Astrophysics, **390** 751 (2002).
- [7] R. Voltz et al, *Journal of Chemical Physics*, **45** (1966) 3306.
- [8] B.S. Nilsen et al., *Fragmentation cross sections of relativistic ^{84}Kr and ^{109}Ag nuclei in targets from hydrogen to lead*, Physical Review C **52** 3277 (1995).

- [9] G.D. Westfall et al., *Fragmentation of Relativistic ^{56}Fe* , Physical Review C **19** 1309 (1979).
- [10] B. Rauch, *Measurement of the relative abundance of the ultra-heavy galactic cosmic rays ($30 \leq Z \leq 40$) with the Trans-Iron Galactic Element Recorder (TIGER) instrument*, PhD Thesis, Washington University, St. Louis 2008.
- [11] <http://www.srl.caltech.edu/ACE/ASC/level2/index.html>
- [12] J.J. Engelmann et al., *Charge composition and energy spectra of cosmic-ray nuclei for elements from Be to Ni. Results from HEAO-3-C2*, Astronomy and Astrophysics **233** 96 (1990).
- [13] A.J. Davis et al., *On the Low Energy Decrease in Galactic Cosmic Ray Secondary/Primary Ratios*", AIP Conference Proceedings **528** 422 (2000).